A NEW ACQUISITION TECHNIQUE FOR CARRIER RECOVERY WITH QAM SIGNALS

P Herbig

ANT Nachrichtentechnik GmbH, Germany

1 ABSTRACT

This paper describes a frequency error detector (FED) for all modulation systems using quadratic modulation schemes, such as 16-QAM, 64-QAM, 256-QAM and so on[1]. Its main advantage is the very high resistance to all kinds of signal faults such as distortions, level errors or noise. Simultaneously, it permits a high acquisition range to be achieved (more than $\Delta f/f_S$ =5% in noise-free environments). Typical applications of the new FED are data transmissions over fading channels without using preambles or other additional helps for carrier acquisition. For this reason, very economical XPIC structures become possible. The method described here can be regarded as an advanced development of the FEDs presented by Sari and Moridi [3].

2 INTRODUCTION

At the beginning of a carriered transmission or after a system outage has occurred, the frequency and phase of the transmitter oscillator have to be estimated at the receive side as quickly as possible. The common approaches for this task consist in either enhancing the bandwidth of the loop filter in the carrier recovery loop or frequency sweeping. While the first method supplies only very few information about the frequency error at high deviations and quickly fails with larger signal defects, the second method generally requires a longer acquisition time.

A more advanced method is implementing a carrier lock detector. The latter has to decide between two operating modes, i.e. the so-called *acquisition mode* as long as the carrier frequency is unknown and the so-called *tracking mode* after the carrier has been caught. In the tracking mode, the usual phase error detector (PED) $(e_I a_Q - e_Q a_I)$ can be further used, with a_I, a_Q for the decision outputs, and e_I, e_Q for the decision errors in the in-phase and quadrature signal path. The PED output is then relevant for small phase errors only, since for greater phase errors, the lock detector activates not the PED, but the FED. In the acquisition mode, the FED should supply as much information about the *frequency error* as possible, but should also provide reliable information about the *phase error* to guarantee a soft switchover to the tracking mode. This paper presents a very simple and effective method to build a FED for quadratic modulation schemes, which exceeds the other ones known to date in distortion resistance.

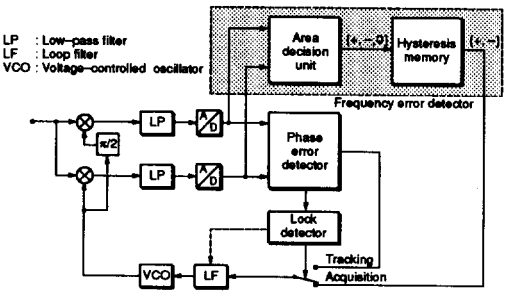

Figure 1: Phase and frequency error detector embedded in a carrier recovery system.

In chapter 3, the method itself is introduced. Afterwards, the FED is analyzed as a random process in chapter 4. An (approximate) model of the FED is presented as a Poisson process. This analysis is accompanied by some simulation results concerning the quality that can be achieved.

Finally, in chapter 5, it is shown that especially the resistance of the new FED to any signal faults is very important for radio systems with reused cross-polarized carriers in combination with economic baseband cross-polarization cancellers (XPICs). A short summary of this paper is given in the very last chapter.

3 FUNCTION

The embedding of a FED in a complete carrier recovery system is shown in **Fig. 1**: The lower part of this figure shows a conventional synchronization loop consisting of the loop filter LF, the voltage-controlled oscillator VCO, the sin/cos modulators and above all the PED, which has to estimate the difference between the actual and the desired value of the demodulation phase. The lock detector LD must identify, whether this loop has locked or not. In case of unlocked carriers, the FED has to assume frequency control.

The FED itself only consists of two parts. The first part is an area decision unit (ADU) working on the

[1] German Patent P 41 00 099.4-31

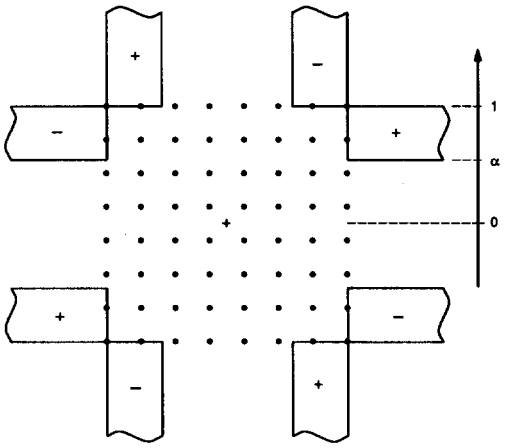

Figure 2: 64-QAM alphabet with the area decision unit of the FED ($\alpha = 4/7$).

basis of the demodulated and sampled receive signals. This part can be considered as a PED with very special characteristics which will be explained later. The second part is a simple hysteresis converting the PED into a FED.

The ADU is shown in **Fig. 2**. This figure shows the complex-valued transmit symbols of a 64-QAM alphabet and outside of it a total of eight bordered areas, four of them being marked with '+' and four of them with '-'. These signs indicate the phase errors (or, better speaking, the signs to adjust the errored phase). The areas are met by the received samples only when the transmit symbols are rotating, i.e. in case of an errored demodulation frequency. α is a parameter adjusting the shape of the decision areas.

The ADU therefore supplies an output signal of $u_{\mathrm{ADU}} = +1$, when areas marked with '+' are met, and an output signal of $u_{\mathrm{ADU}} = -1$, when areas marked with '-' are met. Otherwise it supplies an output signal of $u_{\mathrm{ADU}} = 0$. This structure produces a PED with a static phase plot in compliance with **Fig. 3a**. There the output signal is plot versus phase error φ. Since the QAM modulation scheme is symmetrical with respect to the period of 90 degrees, the phase plot is repeated with the same period.

A frequency error of the demodulator oscillator means rotating input signals and a continually increasing phase error. In this case, the *static phase plot* can also be interpreted as *time plot* of the PED output signal. The average of this signal is vanishing and no information about the frequency is so far obtained. The desired operation as FED instead of a PED is achieved only by inserting a hysteresis into the control path exactly according to the rule: persistence of the effect also after termination of the cause.

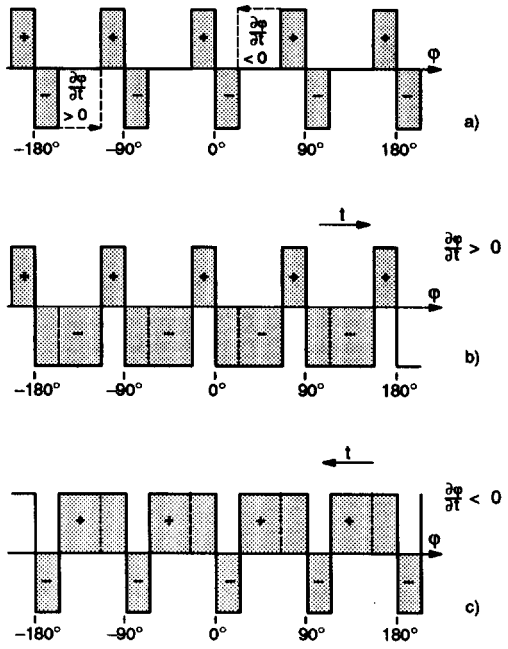

Figure 3: a) Static phase plot of the PED, b) FED output for anti-clockwise signal rotation, c) FED output for clockwise signal rotation.

When assuming an anti-clockwise rotation of the receive signal, the φ axis can be interpreted as *positive* time axis. The FED output signal then keeps the negative value until a new positive cause will force a positive output. This is repeated four times per revolution and produces a FED output *negative* in the average as illustrated in **Fig. 3b**. In the same sense, the φ axis becomes a *negative* time axis with a clockwise signal rotation and the FED output keeps a positive value in the hysteresis memory. **Fig. 3c** shows the FED output which is in this case *positive* in the average. The overall result thus obtained is the wanted frequency error signal out of $\{\pm 1\}$ depending on the sense of signal rotation, with 0 being cancelled by the hysteresis. Finally, the FED output signal has to be passed through the loop filter before the VCO can be controlled.

After capturing the transmitter carrier, the lock-in detector switches over to the tracking mode to activate the normal PED, which then has to track the carrier phase with the lowest possible pattern jitter.

This new method described so far is a combination of the ideas of Aoki et al [1] - who presented in 1984 the *maximum level error algorithm*, which represents an adaptation algorithm for equalizer coefficients and uses only the *outer areas* with *known error signs* - and of Horikawa and Saito [2] - who, as far as I know, used for the first time a hysteresis to set up a FED. Later

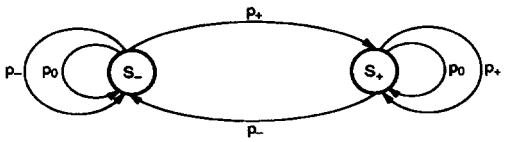

Figure 4: State transition diagram of the *corner tracing* FED.

Sari and Moridi [3] also took up the idea of using a hysteresis to design FEDs for PSK and QAM signals.

The advantage of the new FED, compared to the ones already known, is based on the fact that only the 'corners' of the received symbols are recognized and interpreted. For this reason, we call this the *corner tracing* method. Because even severely distorted signals remain approximate corners, it is possible to detect their sense of rotation. This ensures a high insensitivity to all kinds of distortions.

4 QUALITY

A formal description of the *corner tracing* process is very simple. The FED output signal u_{FED} prevailing at the moment $(n+1)$ is evaluated using the following rule:

$$u_{\mathrm{FED}}(n+1) = \begin{cases} u_{\mathrm{FED}}(n) & \text{if } u_{\mathrm{ADU}}(n) = 0 \\ +1 & \text{if } u_{\mathrm{ADU}}(n) = +1 \\ -1 & \text{if } u_{\mathrm{ADU}}(n) = -1 \end{cases} \quad (1)$$

with $u_{\mathrm{ADU}}(n)$ being the output signal of the ADU prevailing at the moment n. To get a better insight of the operating mode, an analysis is performed using the state diagram as shown in **Fig. 4**. The state machine is not markovian, since the state transition probabilities are depending on the carrier phase φ and are therefore time-variant. These transition probabilities are

$$p_-(\varphi) = \Pr\{u_{\mathrm{ADU}}(\varphi) = -1\} \quad (2)$$

$$p_0(\varphi) = \Pr\{u_{\mathrm{ADU}}(\varphi) = 0\} \quad (3)$$

$$p_+(\varphi) = \Pr\{u_{\mathrm{ADU}}(\varphi) = +1\}. \quad (4)$$

If $S_+(\varphi_n)$ denotes the probability that with a specific phase error φ_n, the state machine is in a state with the output being $+1$ (the average is to be taken over a great number of symbols), and if $S_-(\varphi_n) = 1 - S_+(\varphi_n)$ denotes the other state probability, the following state change relations are applicable:

$$\begin{aligned} S_+(\varphi_n + \Delta\varphi_n) &= S_+(\varphi_n)\,(p_0(\varphi_n) + p_+(\varphi_n)) \\ &\quad + S_-(\varphi_n)\,p_+(\varphi_n) \\ &= S_+(\varphi_n)\,p_0(\varphi_n) + p_+(\varphi_n) \quad (5) \\ S_-(\varphi_n + \Delta\varphi_n) &= S_-(\varphi_n)\,(p_0(\varphi_n) + p_-(\varphi_n)) \\ &\quad + S_+(\varphi_n)\,p_-(\varphi_n) \\ &= S_-(\varphi_n)\,p_0(\varphi_n) + p_-(\varphi_n). \quad (6) \end{aligned}$$

Here it is assumed that the change of one state to the next state occurs in an increase in the phase error of $\Delta\varphi$ with:

$$\Delta\varphi = 2\pi\Delta f / f_S. \quad (7)$$

$\Delta f / f_S$ is the ratio of the carrier frequency error Δf and the symbol rate f_S. In general, the step phase $\Delta\varphi$ does not divide the unit circle by an integer, so that the state probabilities $S_+(\varphi_n)$ and $S_-(\varphi_n)$ are infinite sequences without any periodicities. The average FED output signal is also a function of φ_n:

$$\begin{aligned} &\mathop{\mathrm{E}}_{\mathrm{Symb}}\{u_{\mathrm{FED}}(\varphi_n + \Delta\varphi_n)\} = \\ &= S_+(\varphi_n + \Delta\varphi_n) - S_-(\varphi_n + \Delta\varphi_n) \\ &= (S_+(\varphi_n) - S_-(\varphi_n))\,p_0(\varphi_n) + p_+(\varphi_n) - p_-(\varphi_n) \\ &= \mathop{\mathrm{E}}_{\mathrm{Symb}}\{u_{\mathrm{FED}}(\varphi_n)\} + p_+(\varphi_n) - p_-(\varphi_n). \quad (8) \end{aligned}$$

To get a control signal for the carrier oscillator, the average is to be taken over the time or over a long sequence of phase errors φ_n:

$$\overline{u}_{\mathrm{FED}} = \mathop{\mathrm{E}}_{\varphi_n}\{\mathop{\mathrm{E}}_{\mathrm{Symb}}\{u_{\mathrm{FED}}(\varphi_n)\}\}. \quad (9)$$

The exact evaluation of $\overline{u}_{\mathrm{FED}}$ for arbitrary frequency errors Δf - using e.g. mixed Fourier transformations, series *and* integrals - seems to be very tough, so that a closed solution is omitted here. Only in the lower frequency range, where the discrete time effects can be neglected, a complete solution is possible. Here the random process can be modelled as a Poisson process which permits transitions at any time. In this case, the time index n can be cancelled in the above formulas and all quantities become periodic in φ, including the detector output signal now defined as

$$\overline{u}_{\mathrm{FED}}(\varphi) = \mathop{\mathrm{E}}_{\mathrm{Symb}}\{u_{\mathrm{FED}}(\varphi)\}. \quad (10)$$

A limiting process of (5) and (6) leads to the differential equations

$$\frac{2\pi\Delta f}{f_S}\,S'_+(\varphi) + S_+(\varphi)(1 - p_0(\varphi)) = p_+(\varphi) \quad (11)$$

$$\frac{2\pi\Delta f}{f_S}\,S'_-(\varphi) + S_-(\varphi)(1 - p_0(\varphi)) = p_-(\varphi). \quad (12)$$

These are connectable to only one single differential equation in $\overline{u}_{\mathrm{FED}}(\varphi)$. This detector output signal is a direct result of the state probabilities:

$$\overline{u}_{\mathrm{FED}}(\varphi) = S_+(\varphi) - S_-(\varphi), \quad (13)$$

so that the differential equation in $\overline{u}_{\mathrm{FED}}(\varphi)$ is:

$$\begin{aligned} &\overline{u}'_{\mathrm{FED}}(\varphi) + \frac{f_S}{2\pi\Delta f}\overline{u}_{\mathrm{FED}}(\varphi)(1 - p_0(\varphi)) = \\ &= \frac{f_S}{2\pi\Delta f}(p_+(\varphi) - p_-(\varphi)). \quad (14) \end{aligned}$$

This is a first-order linear differential equation of the general form

$$u' + f(\varphi)u = h(\varphi) \quad (15)$$

with

$$f(\varphi) = \frac{f_S}{2\pi\Delta f}(1 - p_0(\varphi)) = \frac{f_S}{2\pi\Delta f}(p_+(\varphi) + p_-(\varphi)) \tag{16}$$

and

$$h(\varphi) = \frac{f_S}{2\pi\Delta f}(p_+(\varphi) - p_-(\varphi)). \tag{17}$$

The solution of this differential equation is known to be (see e.g. Bronstein and Semendjajew [4]):

$$\overline{u}_{\mathrm{FED}}(\varphi) = [d + \int e^{\int f(\varphi)\,\mathrm{d}\varphi}\, h(\varphi)\,\mathrm{d}\varphi]\, e^{-\int f(\varphi)\,\mathrm{d}\varphi}. \tag{18}$$

Because all signals are periodic with the period of $\varphi = \pi/2$, the constant parameter d is defined by the initial condition:

$$\overline{u}_{\mathrm{FED}}(0) = \overline{u}_{\mathrm{FED}}(\pi/2). \tag{19}$$

This leads to an equation which allows d to be determined:

$$d = [d + \int_0^{\pi/2} e^{\int_0^{\xi} f(\eta)\,\mathrm{d}\eta}\, h(\xi)\,\mathrm{d}\xi]\, e^{-\int_0^{\pi/2} f(\xi)\,\mathrm{d}\xi}. \tag{20}$$

To get the oscillator control signal, which represents the overall aim of these calculations, the average is to be taken from $\overline{u}_{\mathrm{FED}}(\varphi)$ over one period:

$$\overline{u}_{\mathrm{FED}} = \frac{2}{\pi}\int_0^{\pi/2} \overline{u}_{\mathrm{FED}}(\varphi)\,\mathrm{d}\varphi. \tag{21}$$

Unfortunately an evaluation of these formulas is not feasible for realistic state transition probabilities, not even for very simple ones.

For this reason, an approximation solution is envisaged for both the lower and higher frequency error range. In doing so, the state transition probabilities are measured by means of a computer simulation. A 64-QAM modulation scheme is assumed with a signal-to-noise ratio of 10dB, the ADU parameter α being set to 4/7. The results $p_-(\varphi)$, $p_+(\varphi)$, their sum, their difference (see equations (16) and (17)) and the resulting detector output signal $\overline{u}_{\mathrm{FED}}(\varphi)$ for a frequency error of $\Delta f/f_S = 5 \cdot 10^{-4}$ are plotted in **Fig. 5** for the phase range of $-45°$ to $+45°$. In this example, the average FED output is $\overline{u}_{\mathrm{FED}} = -0.077$. Since a small positive frequency error Δf is assumed, the average of the correction signal must be negative.

Obviously the following model matches these figures very well:

$$h(\varphi) = -\frac{f_S}{2\pi\Delta f} a_1 \sin 4\varphi, \tag{22}$$

$$f(\varphi) = \frac{f_S}{2\pi\Delta f}(a_2 + a_3 \cos 4\varphi). \tag{23}$$

a_1, a_2 and a_3 are parameters depending on the signal-to-noise ratio and the ADU parameter α. In the appendix, it is shown that the following approximation is applicable in this model for $\Delta f \to 0$:

$$\overline{u}_{\mathrm{FED}} \approx -\frac{2\pi\Delta f}{f_S}\frac{2a_1a_3}{(a_2^2 - a_3^2)^{1.5}}. \tag{24}$$

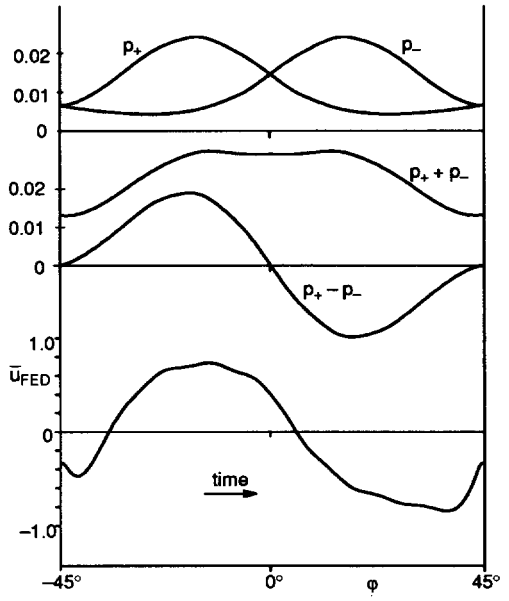

Figure 5: State transition probabilities, functions of (16) and (17) and $\overline{u}_{\mathrm{FED}}(\varphi)$ for $\Delta f/f_S = 5 \cdot 10^{-4}$.

Since the FED output is vanishing for $\Delta f \to 0$, the FED must also be an appropriate PED. Otherwise there will be problems when the system switches from the acquisition mode to the tracking mode, because $\Delta f \approx 0$ will always prevail during switchover. It would be possible, for example, to improve the original FED *corner tracing* performance in the high-noise and low-frequency range by increasing the memory depth of the hysteresis. Since, however, the PED characteristic is violated by this procedure, the complete system performance will not be enhanced.

In the appendix, another approximative solution is drawn up for the high frequency error range:

$$\overline{u}_{\mathrm{FED}} \approx -\frac{f_S}{2\pi\Delta f}\frac{a_1a_3}{8a_2}. \tag{25}$$

In this case, the FED output is vanishing for $\Delta f \to \infty$. Of course, this result has to be handled with care, since the Poisson model is no longer valid for higher frequency errors. Thus, the maximum frequency error detectable using the *corner tracing* procedure is of course finite.

Some simulations were run with arbitrary frequency errors to evaluate the transition and state probabilities for a specific error phase. There is no longer a cyclic $\overline{u}_{\mathrm{FED}}(\varphi)$, because its value now depends to a large extent on the past. Thus, the recursion equations (5) and (6) or directly (8) have to be evaluated using a long sequence of φ_n. The results of this simulation process are presented below. **Fig. 6** shows the detector output

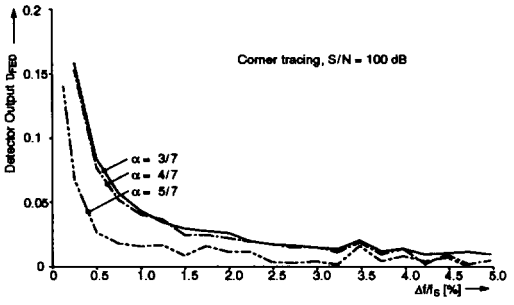

Figure 6: Detector output of the *corner tracing* FED for noise-free 64-QAM symbols.

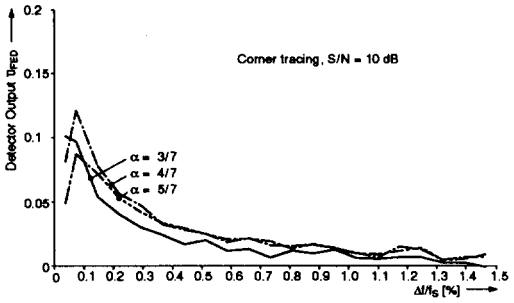

Figure 7: Detector output of the *corner tracing* FED for 64-QAM symbols with $S/N = 10$ dB.

$\overline{u}_{\mathrm{FED}}$ over the frequency error $\Delta f/f_S$ in terms of the percentage rate. The symbols assumed here are noise-free samples of a 64-QAM alphabet. The parameter α is set to 3/7, 4/7 and 5/7. Very similar characteristics are achieved with $\alpha = 3/7$ and $\alpha = 4/7$. The results with $\alpha = 5/7$ are a somewhat worse. Thus, it becomes obvious that *corner tracing* is more than only evaluating the single corner symbol. However, the results are not very sensitive regarding the correct choice of α. Of course, the information decreases with higher frequency errors, but values of 5% and more can be reached. In a realized 64-QAM system with a data rate of 160 MBit/s, a lock-in range of about 2 MHz was measured. This corresponds to a ratio of $\Delta f/f_S = 7.5\%$.

The simulation results for finite signal-to-noise ratios are much more interesting. A ratio of $S/N = 10$ dB means e.g. a very strong distortion in a 64-QAM system, exemplary for all kinds of signal faults. The results up to a maximum frequency error of $\Delta f/f_S = 1.5\%$ are shown in **Fig. 7**. The best performance for high acquisition ranges in noise-free environments and strong signal distortions are achieved with $\alpha = 4/7$. Fig. 7 also documents the resistance stated above.

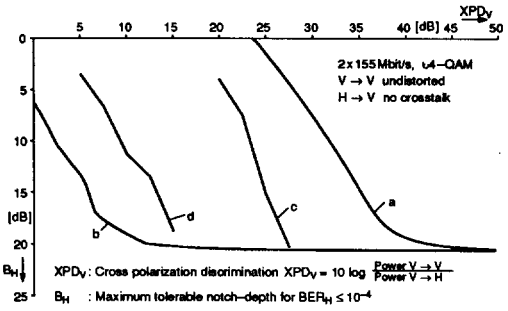

Figure 8: Signatures for a cross-polarized 64-QAM system, a) lock-out without decoupler, b) lock-out with 9-tap decoupler, c) lock-in with standard method, d) lock-in with *corner tracing*.

5 APPLICATION

Typical applications of the new FED are microwave radio systems with transmission channels severely distorted due to multipath propagation in broadband systems or due to rainfall in systems using higher radio frequencies.

When highspeed broadband systems are distorted by multipath propagation, adaptive filters are required to equalize intersymbol interference. Furthermore, systems transmitting two independent signals in a cross-polarized way need additional adaptive filters to decouple the interference of the cross-polarized signal.

In systems with one single polarization and thus an equalizer only, there are normally no serious problems regarding the general acquisition. Since the equalizer is very well able to adapt its coefficients even with rotating input signals, the carrier recovery unit can wait until the equalizer has equalized the channel. For an example, refer to Herbig et al. [5]. Hence, the standard lock-in procedure is: first the equalizer, then the carrier. Nevertheless, *corner tracing* may reduce the system outage times.

In economical and hardware-efficient cross-polarized receivers with the correction signal being extracted after the demodulation, the situation is completely different. There the filters are not able to adapt their coefficients before *both* carriers have been caught. Thus, the lock function for carrier recovery must cover the widest possible channel dispersion range. Moreover, the resistance of the FED to all kinds of interference signals becomes an important and very critical quantity for the lock-in behaviour.

Fig. 8 compares the lock-in signatures of a cross-polarized 2x155 Mbit/s 64-QAM system. Cross-coupling in only one direction is assumed (from the vertical to the horizontal path) with a delay of 6.3ns. The co-polarized (horizontal) channel is distorted by

multipath fading with the notch in the band center and an echo delay of also 6.3ns. The vertical channel is assumed to be free from distortion. The curves depicted in Fig. 8 show the maximum permissible cross-polarization discrimination XPD_V versus the notch-depth B_H in the horizontal path. In this connection, the term maximum permissible means a bit error rate of $BER_H = 10^{-4}$. **Fig. 8a** represents the system performance without decoupling the crosstalk signal (lock-out signature): only a very little crosstalk signal is allowed. Activating the decoupler (**Fig. 8b**, 9 linear taps with parallel equalizer) improves this lock-out signature by about 29 dB regarding the XPD_V value. However, acquisition is very poor with standard methods. This is shown in **Fig. 8c** which represents the lock-in signature of a usual PED with enlarged loop bandwidth during acquisition. The last curve, i.e. **Fig. 8d**, shows the lock-in signature of the *corner tracing* method. Concerning the channel distortions assumed here, the lock-out signature is not perfectly matched, but an improvement of 13.5 dB is reached regarding the XPD_V value. Thus, in most cases acquisition can be guaranteed.

6 CONCLUSION

A new frequency error detector for QAM alphabets has been presented. Its main advantage is the high resistance to all kinds of signal faults. It has been shown that an acquisition range of more than $\Delta f/f_S = 1\%$ can be reached without any problems for a noisy 64-QAM signal with a signal-to-noise ratio of 10dB (in noise-free environments more than $\Delta f/f_S = 5\%$). Since the new method recognizes particularly the corners of the received alphabet, we are talking about a *corner tracing* detector. To perform a detailed analysis, the detection process was modelled as a Poisson process. A general solution could be found and the results derived therefrom were compared to several simulations executed before.

A APPENDIX

For $\Delta f = 0$, the derivative $\overline{u}'_{FED}$ is vanishing in (14) and a first approximation for $\overline{u}_{FED}$ is represented by

$$\overline{u}_{FED}|_{\Delta f=0} = \frac{h}{f}. \tag{26}$$

This equation is the starting point to get a second approximation for $\Delta f \to 0$ by solving equation (14) to achieve $\overline{u}_{FED}$:

$$\overline{u}_{FED}|_{\Delta f\to 0} \approx \frac{h - \overline{u}'_{FED}|_{\Delta f=0}}{f} = \frac{h - (\frac{h}{f})'}{f}. \tag{27}$$

To get the average FED output, this equation has to be integrated over one period. Because of the symmetries of f and h (see Fig. 5), it can be shown that the integral is reducible to:

$$\overline{u}_{FED} \approx \frac{1}{\pi}\int_0^{\pi/2} \frac{h'}{f^2}\,\mathrm{d}\varphi. \tag{28}$$

With the models (22) and (23), this integration results in

$$\overline{u}_{FED} \approx -\frac{2\pi\Delta f}{f_S}\frac{2a_1a_3}{(a_2^2 - a_3^2)^{1.5}}. \tag{29}$$

To fit the plots of Fig. 5, the parameters have to be set to $a_1 = 0.02$, $a_2 = 0.023$ and $a_3 = 0.007$. This leads to $\overline{u}_{FED} \approx -170\Delta f/f_S$. This can be easily verified using Fig. 7. The frequency error $\Delta f/f_S = 5 \cdot 10^{-4}$ (as assumed in Fig. 5) results in $\overline{u}_{FED} = -0.085$. This result is nearly identical with the direct evaluation result (see above).

In the high frequency error range ($\Delta f \to \infty$), the e-function of (20) can be replaced by an abandoned power series with neglected high-order terms. The initial value d then becomes

$$d = \frac{f_S}{2\pi\Delta f}\frac{a_1}{4}(1 - \frac{a_3}{2a_2}), \tag{30}$$

and the essential parts of $\overline{u}_{FED}(\varphi)$ are

$$\overline{u}_{FED}(\varphi) = -\frac{f_S}{2\pi\Delta f}(\frac{a_1a_3}{8a_2} - \frac{a_1}{4}\cos 4\varphi + \ldots). \tag{31}$$

Finally, the integral over one period results again the average FED output:

$$\overline{u}_{FED} \approx -\frac{f_S}{2\pi\Delta f}\frac{a_1a_3}{8a_2}. \tag{32}$$

With the parameters matching Fig. 5, this results in $\overline{u}_{FED} \approx -1.2 \cdot 10^{-4} f_S/\Delta f$. This can be verified also using Fig. 7.

REFERENCES

1. Aoki, K., Yamada, H., Ikuta, K., Takenaka, S. and Daido Y., 1984. IEEE Inter. Conf. on Comm., 1003-1006.

2. Horikawa, I. and Saito, Y., 1980. Trans. IECE Japan, 63-B, 692-699.

3. Sari, H. and Moridi S., 1988. IEEE Trans. on Comm., 36, 1035-1043.

4. Bronstein, I.N. and Semendjajew, K.A., 1973. "Taschenbuch der Mathematik", Verlag Harri Deutsch, Zürich und Frankfurt/Main, 378.

5. Herbig, P., Elser, M. and Ottka, M., 1991. Europ. Conf. on Radio Relay Systems, 378-385.